Trop J Nat Prod Res, September 2025; 9(9): 4553 - 4562 **ISSN 2616-0684 (Print)**
ISSN 2616-0692 (Electronic)

Tropical Journal of Natural Product Research

Available online at https://www.tjnpr.org

Original Research Article

Anticancer Activity of Combined Extracts of Sappan Wood (*Caesalpinia sappan* L.) and Coffee Stem Parasite (*Loranthus ferrugineus* Roxb) Against MCF7 Breast Cancer Cells Through *In Silico* and *In Vitro* Approaches

Tita Juwitaningsih[1]*, Destria Roza[1], Eddiyanto Eddiyanto[1], Murniaty Simorangkir[1], Dwi Sapri Ramadhan[1], Yaya Rukayadi[2]

[1]*Department of Chemistry, Faculty of Mathematics and Natural Sciences, Universitas Negeri Medan, Medan 20221, Indonesia.*
[2]*Lab. of Natural Products, Institute of Bioscience, Universiti Putra Malaysia, 43400 UPM Serdang, Selangor Darul Ehsan, Malaysia*

ARTICLE INFO

Article history:
Received 11 June 2025
Revised 04 September 2025
Accepted 07 September 2025
Published online 01 October 2025

ABSTRACT

Breast cancer remains the most prevalent malignancy among women worldwide. Adverse side effects associated with conventional cancer therapies have driven the search for alternative chemopreventive agents from natural sources. *Caesalpinia sappan* L. and *Loranthus ferrugineus* Roxb. have long been used in traditional medicine and possess anticancer properties. This study aimed to evaluate the anticancer activity of single and combined extracts of *C. sappan* L. and *L. ferrugineus* Roxb. against Michigan Cancer Foundation-7 (MCF-7) breast cancer cells and elucidate their molecular mechanisms via *in silico* docking simulations. *In silico* screening focused on brazilin and quercetin, the principal phytoconstituents of *C. sappan* L. and *L. ferrugineus* Roxb., respectively, compared with a standard drug targeting cytochrome P450 3A4 (CYP3A4, PDB ID: 1TQN) using PyRx AutoDock Vina. The resazurin reduction assay was used to determine in vitro cytotoxicity against MCF-7 cells using acetone extracts of *L. ferrugineus* Roxb., *C. sappan* L., and their combinations at ratios of 1:1, 2:1, and 1:2. *In silico* results indicated that brazilin and quercetin complied with Lipinski's Rule of Five, with binding affinities of −8.2 kcal/mol and −8.9 kcal/mol, respectively, whereas their combination violated the rule. While both compounds individually exhibited promising anticancer potential, their combination showed a competitive antagonistic effect. *In vitro* findings showed that *C. sappan* L. extract exerted moderate cytotoxicity (IC_{50} = 56.21 µg/mL), whereas *L. ferrugineus* Roxb. extract had an IC_{50} of 112.9 µg/mL. All extract combinations were inactive, indicating antagonistic interactions between the secondary metabolites of both plants.

Keywords: Anticancer activity, *Caesalpinia sappan*, *Loranthus ferruginueus*, Michigan Cancer Foundation-7 breast cancer cells, Molecular docking

Introduction

Women are among the populations with the highest risk of developing cancer, with breast cancer ranking as the most common malignancy affecting Indonesian women, along with cervical, lung, colorectal, and liver cancers.[1] The primary objectives of cancer treatment are to eliminate malignant cells, control tumor growth, and prevent metastasis.[2] Conventional therapeutic modalities, including chemotherapy, radiotherapy, and surgery, have limitations and adverse side effects. Chemotherapeutic agents, such as cisplatin, paclitaxel, carboplatin, vincristine, and bleomycin, often yield suboptimal outcomes because of their non-specific mechanisms of action and inability to induce programed cell death. Radiotherapy may damage normal tissues and is frequently ineffective for certain tumor types, whereas surgery is unsuitable for metastatic cancers.[3]

*Corresponding author. Email: juwitaningsih@unimed.ac.id
Tel: + 62 812-6522-646

Citation: Juwitaningsih T, Roza D, Eddiyanto E, Simorangkir M, Ramadhan DS, Rukayadi Y. Anticancer Activity of Combined Extracts of Sappan Wood (*Caesalpinia sappan* L.) and Coffee Stem Parasite (*Loranthus ferrugineus* Roxb) Against MCF7 Breast Cancer Cells Through *In Silico* and *In Vitro* Approaches. Trop J Nat Prod Res. 2025; 9(9): 4553 – 4562 https://doi.org/10.26538/tjnpr/v9i9.58

Official Journal of Natural Product Research Group, Faculty of Pharmacy, University of Benin, Benin City, Nigeria

These limitations have prompted the search for alternative chemopreventive agents derived from natural sources, which may inhibit abnormal cell growth with reduced toxicity and improved safety profiles. *Caesalpinia sappan* L., commonly known as sappan wood and locally called "secang" in Indonesia, and *Loranthus ferrugineus* Roxb., commonly known as coffee stem parasite and locally called "benalu kopi," are two medicinal plants traditionally used for various ailments and reported to possess anticancer properties. *C. sappan* L. exhibits cytotoxic activity against lung (A549),[4,5] cervical,[6] breast,[7] and colorectal cancer cell lines.[8] Similarly, *L. ferrugineus* Roxb. has demonstrated activity against cervical (HeLa)[9] and prostate cancer cells.[10] However, the anticancer potential of combining extracts from these two plants remains unexplored; no published studies have investigated the simultaneous docking of their major flavonoids against a common molecular target or receptor.

Flavonoids are the predominant secondary metabolites in *C. sappan* L. and *L. ferrugineus* Roxb. and are known to confer diverse health benefits, including promising roles in cancer prevention and therapy.[11] Brazilin and brazilein, the major bioactive compounds of *C. sappan* L., exert pro-apoptotic effects by downregulating the anti-apoptotic protein survivin, thereby promoting caspase-9 and caspase-3 activation, followed by PARP cleavage, resulting in intrinsic apoptotic cell death in various cancer cell lines.[12–14] Molecular docking studies have demonstrated the binding interactions between flavonoid-like compounds and CYP3A4, indicating that these phytochemicals can occupy and stabilize within the enzyme's active site.[15] CYP3A4 plays a crucial role in the metabolism of several anticancer agents, including the bioactivation of the prodrug cyclophosphamide into its cytotoxic metabolite, 4-hydroxycyclophosphamide, while also contributing to inactivation pathways via N-dechloroethylation, which generate toxic

byproducts such as acrolein and chloroacetaldehyde.[16,17] Ikawati et al. (2020) further reported that the molecular docking of brazilin and brazilein indicated potential inhibitory effects on breast cancer cell proliferation and metastasis.[18]

Quercetin, a major flavonoid in *L. ferrugineus* Roxb., showed potent cytotoxicity against breast (T47D) and cervical (HeLa) cancer cell lines, with IC_{50} values of 9.58 and 3.66 µg/mL, respectively, classifying it as a strong cytotoxic agent.[19,20] Beyond its cytotoxic potency, quercetin exerts multiple anticancer mechanisms, including apoptosis induction, cell cycle arrest, angiogenesis inhibition, and modulation of key signaling pathways such as PI3K/Akt and MAPK.[21,22] When considered alongside brazilin and brazilein, the principal flavonoids from *C. sappan* with well-documented pro-apoptotic and antiproliferative activities, the combination of these phytochemicals presents a compelling rationale for therapeutic exploration. Combining flavonoids from *C. sappan* L. and *L. ferrugineus* Roxb. was hypothesized to potentially exert synergistic or antagonistic anticancer effects, thereby warranting comprehensive evaluation through *in silico* and *in vitro* approaches.

Materials and Methods

Plant Collection and Identification

The dried heartwood of *C. sappan* L. and the dried leaves of *L. ferrugineus* Roxb. were purchased in June 2024 from Sempurna Herbal Medicine Store, Medan, Indonesia (3°35'26.7"N, 98°41'11.2"E). The botanical identity of *L. ferrugineus* was authenticated as *Scurrula ferruginea* (Roxb. ex Jack) Danser (synonym: *Loranthus ferrugineus*), commonly known as coffee stem parasite. The botanical identity of *C. sappan* L. was authenticated as *Biancaea sappan* (L.) Tod (synonym: *Caesalpinia sappan*), commonly known as sappanwood. The taxonomic authentication was conducted at the Herbarium Medanense, University of Sumatera Utara, Medan, Indonesia by Prof. Dr. Etti Sartina Siregar, and voucher specimen were deposited with the following accession numbers: *C. sappan* (No. 1131/MEDA/2025) and *L. ferrugineus* (No. RG4664).

Extraction of Plant Materials

Each plant material was processed separately. The samples were air-dried, ground into a fine powder, and extracted by maceration using redistilled acetone. For each extraction, 500 g of powdered material was immersed in 1500 mL of acetone for 72 hours at room temperature with occasional stirring. The mixture was filtered, and the solvent was renewed every 24 hours to ensure complete extraction. The filtrates were pooled and concentrated under reduced pressure at 45 °C using a rotary evaporator (Catalogue No. R100, Büchi, Flawil, Switzerland) until free of solvent.

To preserve the individual phytochemical profiles, the extractions were performed in separate batches before being combined. Subsequently, three extract combinations of *L. ferrugineus* Roxb. and *C. sappan* L. were prepared in ratios of 1:1, 2:1, and 1:2 (w/w) for further analysis.

In Silico Analysis

The 3D structure of cytochrome P450 3A4 (CYP3A4, PDB ID: 1TQN) was retrieved from the Protein Data Bank (https://www.rcsb.org/). The receptor structure was prepared using PyMOL 2.5 (Schrödinger, LLC) by removing the co-crystallized ligands and water molecules and then adding polar hydrogen atoms. The ligand structures of brazilin, brazilein, and quercetin were obtained in 3D SDF format from the PubChem database (https://pubchem.ncbi.nlm.nih.gov) and geometry-optimized using the Open Babel module in PyRx 0.9.9. To ensure drug-likeness and safety profiles, preliminary ligand screening was performed based on Lipinski's Rule of Five and toxicity prediction using SwissADME (http://www.swissadme.ch/).

Receptor and ligand files were converted to the PDBQT format in PyRx, and the docking grid box was centered on the heme Fe atom with the following coordinates: center X: −16.149, Y: −22.294, Z: −11.431 Å; dimensions X: 15.831, Y: 22.013, Z: 18.481 Å. Molecular docking was performed using AutoDock Vina 1.1.2 integrated in PyRx with the exhaustiveness set to 8.

Method validation was performed through a redocking procedure in which the native co-crystallized ligand of CYP3A4 was redocked into the binding pocket using the same docking parameters. The resulting binding pose was compared with the original crystallographic pose to calculate the root mean square deviation (RMSD). An RMSD value ≤ 2.0 Å was considered indicative of a reliable docking protocol, consistent with established validation standards.[23]

The docking results were evaluated based on the binding free energy (ΔG, kcal/mol) and ligand orientation within the active site of the receptor. Discovery Studio Visualizer v21.1.0 (BIOVIA, Dassault Systèmes) was used to generate 2D and 3D interaction visualizations to identify the key amino acid residues involved in hydrogen bonding, hydrophobic interactions, and π-related interactions.

In vitro assay

Anticancer activity was evaluated using the resazurin reduction method as previously described.[24,25] Human breast cancer cells (MCF-7; ATCC® HTB-22™, Manassas, VA, USA) were used as the target cell line.

Cell culture

Michigan Cancer Foundation-7 (MCF-7) cells were seeded into 96-well plates (Nest 701001, Jiangsu, China) and cultured in Roswell Park Memorial Institute Medium (Gibco 11875-093, New York, USA) supplemented with 10% fetal bovine serum (Gibco 10270-106, New York, USA). Cultures were maintained at 37°C in a humidified incubator with 5% CO_2 (Thermo Fisher Scientific 8000DH, Waltham, MA, USA) until cell confluence reached approximately 70%.

Cytotoxicity assay

Cells were treated for 48 h with various concentrations (1000, 500, 250, 125, 62.5, 31.25, 15.63, and 7.81 µg/mL) of either individual extracts or pre-prepared binary combinations of L. ferrugineus and C. sappan at ratios of 1:1, 2:1, and 1:2 (w/w). After incubation, PrestoBlue™ reagent (Thermo Fisher Scientific A13261, Waltham, MA, USA) was added to each well, and the plates were further incubated under the same conditions. Cisplatin (EDQM C2210000, Strasbourg, France) was used as the positive control. Absorbance was measured using a multimode reader (Tecan M200 Pro, Männedorf, Switzerland) at 600 nm (blue) and 570 nm (pink). Corrected absorbance values were plotted against the sample concentration (µg/mL), and the half-maximal inhibitory concentration (IC_{50}) was calculated from the linear regression equation ($y = a + bx$).

Results and Discussion

In Silico Approach: Drug-likeness and ADME Prescreening

Brazilin and quercetin satisfied Lipinski's Rule of Five with zero violations and exhibited high predicted gastrointestinal absorption, no blood–brain barrier permeability, and bioavailability scores of 0.55, supporting their suitability for further docking evaluation (Table 1). These findings are consistent with established thresholds for orally drug-like molecules (MW ≤ 500 Da, HBD ≤ 5, HBA ≤ 10, logP ≤ 5) and with Veber's criteria (TPSA ≤ 140 Å²; rotatable bonds ≤ 10), which collectively predict acceptable passive permeability and oral bioavailability.[26–29] The TPSA values of brazilin (90.15 Å²) and quercetin (131.36 Å²) fall within the ranges associated with favorable absorption profiles.[30]

CYP3A4 binding pocket context

Docking targeted CYP3A4 (PDB ID: 1TQN), whose active-site cavity is unusually large and malleable, enabling accommodation of bulky substrates and multiple binding modes. The cavity "roof" is formed by SRS-2 and SRS-3 above the heme, while residues proximal to the Fe–heme (e.g., Arg212, Phe108, Phe215, Ala305, Thr309, Ala370, Ile369, and Cys442) frequently mediate ligand recognition and stabilization.[31,32] These structural features rationalize the ability of polyphenolic flavonoids to form mixed networks of hydrogen bonds, π–π contacts, and hydrophobic interactions near the catalytic center.

Table 1. Predicted drug-likeness and ADME profiles of brazilin and quercetin (SwissADME).

Compound	Brazilin	Quercetin
Formula	C16H14O5	C15H10O7
MW	286.28	302.24
H-Bond Acceptor (HBA)	5	7
H-Bond Donor (HBD)	4	5
Rotatable Bonds	0	1
TPSA (Å²)	90.15	131.36
LogP	1.51	1.23
GI Absorption	High	High
BBB Permeant	No	No
Lipinski Violations	0	0
Bioavailability Score	0.55	0.55

Abbreviations: MW, molecular weight (Da); HBA/HBD, hydrogen-bond acceptor/donor; TPSA, topological polar surface area (Å²); logP, consensus logP; GI, gastrointestinal; BBB, blood–brain barrier.

Docking outcomes and binding-mode analysis

Consistent with the ADME screen, AutoDock Vina predicted favorable binding for both ligands (Table 2). Quercetin showed the most negative binding free energy (ΔG = −8.9 kcal/mol), followed by brazilin (−8.2 kcal/mol) and the reference tamoxifen (−7.9 kcal/mol). The quercetin pose established polar contacts within the active site (e.g., THR310, PRO434 backbone, and ALA370) and additional proximity contacts near CYS442 and the heme surface (Figure 1), consistent with the inhibitory occupancy close to the catalytic iron; thus, it has potential as an inhibitory agent, as reported by Tang et al. (2023), in which quercetin has been shown to function as a breast cancer inhibitor.[33] Brazilin formed hydrogen bonds with ALA305 and ARG212 (Figure 2) and hydrophobic contacts in the heme-adjacent pocket, which was also compatible with inhibitory binding. The relative ranking (quercetin < brazilin < tamoxifen) reflects stronger predicted interaction networks and favorable orientation within SRS-defined regions above the heme.[31,32,34]

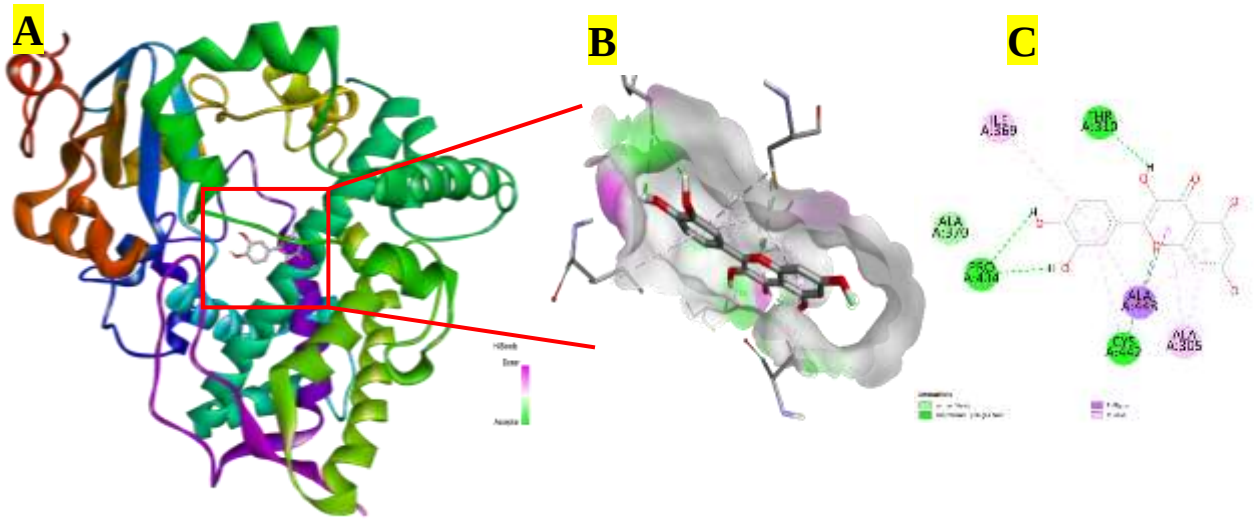

Figure 1. Quercetin–CYP3A4 complex. (A) Quercetin in the CYP3A4 pocket near the heme; (B) 3D interaction map highlighting H-bond donor/acceptor surfaces; (C) 2D interaction diagram showing H-bonding to THR310 and PRO434 and contacts near CYS442 and ALA370

Figure 3 shows that tamoxifen binds primarily through hydrophobic contacts with PHE108, PHE215, and ALA370, lacking the extensive hydrogen bonding seen in quercetin and brazilin; this interaction pattern supports its stable packing above the heme but with less flexibility for multi-point anchoring.

Interpretation and linkage to pocket chemistry

Residues such as ALA370, PHE108/PHE215, and CYS442 are frequently implicated in the hydrophobic packing and positioning of ligands near the catalytic iron; contacts with these residues are commonly observed among diverse CYP3A4 ligands and inhibitors.[35–37] The quercetin pose, which is rich in hydroxyl and carbonyl groups, supports a mixed H-bond/hydrophobic binding pattern, whereas brazilin relies on fewer H-bond donors/acceptors with efficient packing, explaining its slightly weaker ΔG in the system. This pattern mirrors previous structural analyses that attribute CYP3A4's ligand promiscuity to its voluminous, flexible cavity and multiple access/exit channels, enabling alternative orientations and contact networks.[36,37]

QSAR-informed implications for the combined-ligand model

The merged-ligand model (brazilin + quercetin) displayed MW (≈555 Da), volume, and surface area well beyond typical drug-like ranges (Table 3). Exceeding RO5/Veber thresholds, such as high MW/SA and borderline lipophilicity, is expected to reduce passive permeability and can hinder optimal packing within the cavity, especially beneath the SRS-2/SRS-3 "roof," thereby disfavoring a stable pose.[26,27,30] This aligns with the less favorable docking behavior of the merged model and is consistent with the antagonistic effects observed *in vitro* for extract combinations. While Vina permits single-ligand docking, the standard protocol does not model the simultaneous co-docking of two separate small molecules, and steric and entropic penalties would likely disfavor such a merged construct in reality.[28]

Docking protocol reliability was established via redocking methods using the accepted RMSD ≤2.0 Å criterion to assess pose reproduction. The following standard caveats apply: Vina scores have an estimated error on the order of a few kcal/mol; therefore, trends are more meaningful than absolute values.

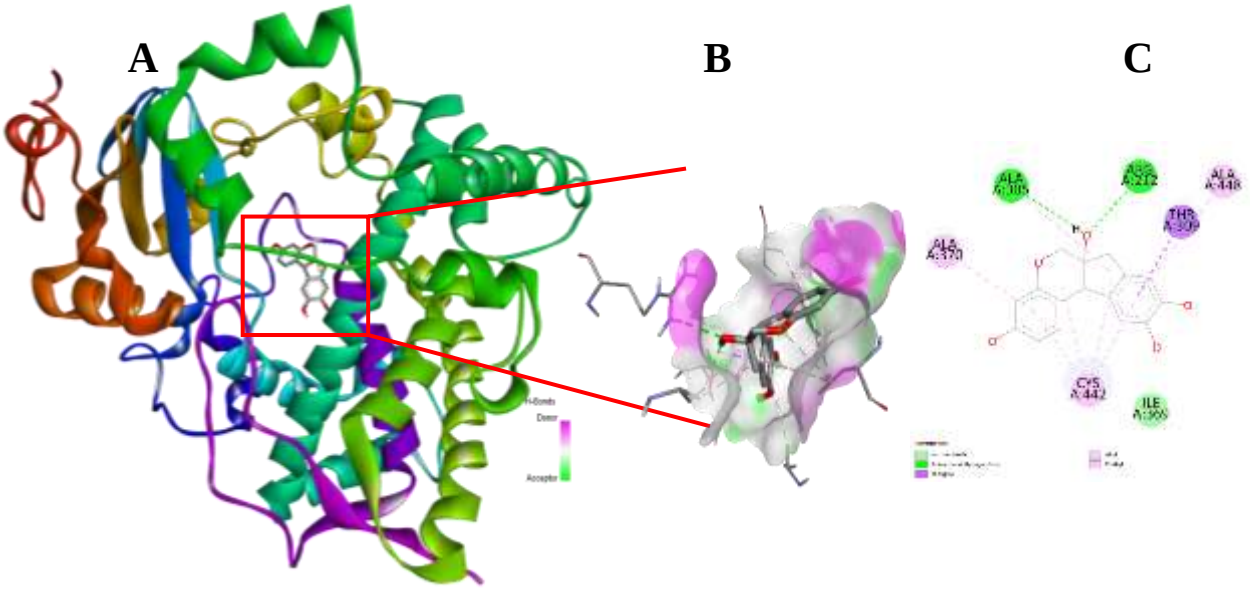

Figure 2. Brazilin–CYP3A4 complex. (A) Brazilin in the active site; (B) 3D interaction map; (C) 2D interaction diagram showing H-bonding to ALA305 and ARG212 and hydrophobic packing near the heme

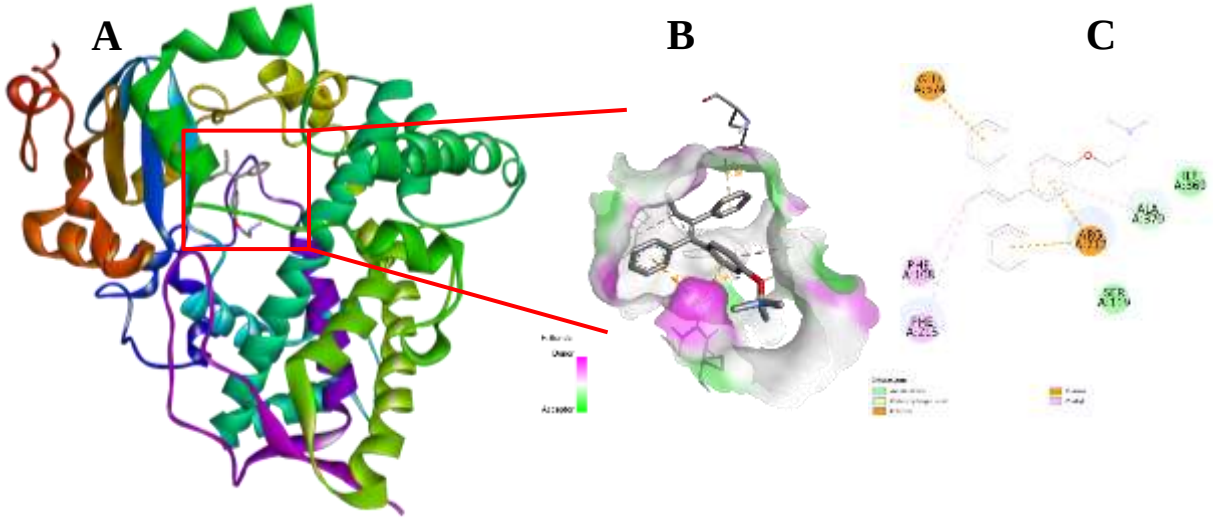

Figure 3. Tamoxifen–CYP3A4 complex used as a reference ligand. (A) Binding orientation relative to SRS-"roof" residues PHE108/PHE215; (B) 3D interaction map; (C) 2D interaction diagram.

The combined brazilin–quercetin ligand failed to meet Lipinski's Rule of Five owing to an excessive molecular weight (>500 Da) and large surface area, which likely hindered passive membrane diffusion and diminished oral bioavailability.[26] Its oversized molecular volume also impaired the binding efficiency, as bulky ligands often struggle to fit optimally within the CYP3A4 active site. Although its log P remained below 5, it exceeded the ideal oral drug range of 1.35–1.8, indicating excessive hydrophobicity that may reduce receptor selectivity. Furthermore, reduced hydration energy implies poor aqueous solubility and compromised membrane transport. Notably, nanotechnology offers practical solutions: nanoencapsulation, such as lipid-based nanoparticles, polymeric carriers, or nanostructured lipid systems, has been shown to enhance the solubility, stability, and bioavailability of phytochemicals, such as quercetin, enabling improved intracellular delivery and therapeutic efficacy.[38,39] Consequently, while the native brazilin–quercetin combination violates key drug-like properties, advanced nanodelivery strategies could still capitalize on its pharmacological potential.

Based on the QSAR parameters, the combined brazilin–quercetin model exceeded the optimal molecular weight and surface area thresholds, which is expected to cause steric and permeability limitations in CYP3A4 binding. This physicochemical incompatibility may contribute to the antagonistic interaction and lack of anticancer activity observed *in vitro*, despite favorable single-ligand docking profiles (Figures 1–3).

In Vitro Cytotoxicity Assay

This study quantified cell viability using the resazurin (7-Hydroxy-3H-phenoxazin-3-one-10-oxide) reduction assay (PrestoBlue™), which reports metabolic competence through the enzymatic conversion of oxidized resazurin (blue, non-fluorescent) to resorufin (pink, fluorescent) by intracellular electron carriers NADH/NADPH/FADH

Table 2. AutoDock Vina docking results for quercetin, brazilin, and tamoxifen against CYP3A4 (PDB ID: 1TQN)

Ligand	ΔG (kcal/mol)	Amino Acid Residu	Distance (Å)
Quercetin	-8.9	PRO434, THR310, CYS442, ALA448, ALA305, ILE369	PRO434(2,47), PRO434(2,65), THR310(2,04), ALA370(2,33), CYS442(3,39)
Brazilin	-8.2	ALA305, ARG212, THR309, CYS442, ALA448, ALA370	ALA305(2,62), ARG212(2,69)
Tamoxifen	-7.9	ALA370, ARG212, GLU374, PHE108, PHE215	ALA370 (2.96)

Abbreviations: ΔG, binding free energy; Å, ångström.

via mitochondrial and cytosolic oxidoreductases. Therefore, the signal inversely correlates with cytotoxicity.[40] Figure 4 illustrates this conversion. The observed change in color/absorbance was used to generate linear regression plots for the dose–response calculations. Figure 5 presents the linear regression graph of the *L. ferrugineus* Roxb and *C. sappan* L. extracts.

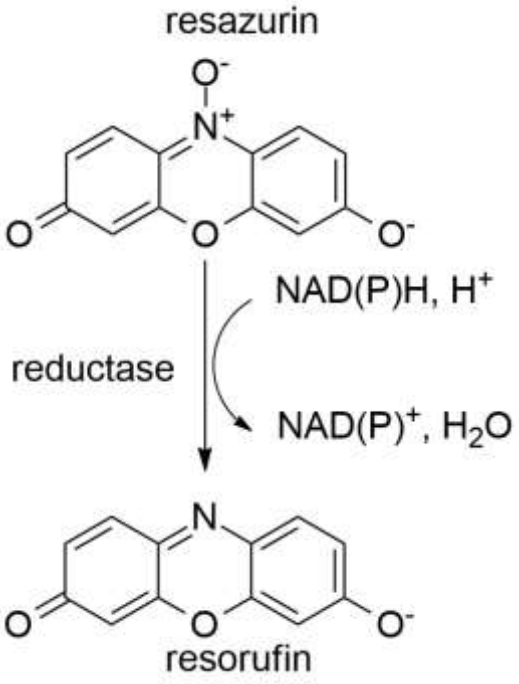

Figure 4. Resazurin–resorufin conversion underlying the viability assay.[40]

Effectiveness of individual extracts

Linear regression from Figure 5a and b yielded IC_{50} values of 112.9 µg/mL for the acetone extract of *L. ferrugineus* and 56.21 µg/mL for *C. sappan*. Interpreting these data with commonly used NCI-derived thresholds where crude extracts with GI_{50}/IC_{50} ≤30 µg/mL are considered promising/strongly cytotoxic, and values ≤100 µg/mL are often deemed to exhibit moderate activity, and is regarded as inactive when the IC_{50} value is greater than 100 µg/mL.[41] This study shows that *C. sappan* is moderately active, whereas *L. ferrugineus* is inactive in this model.

Morphological documentation (Figure 6a and b) supports these findings: at 62.50 µg/mL, *L. ferrugineus* reduced the viable-cell density, fewer bright nuclei, and membrane compromise, whereas *C. sappan* at 31.25–62.50 µg/mL produced a marked loss of viable morphology, approaching the cisplatin control phenotype.

Previous studies reported that the acetone extract of *L. ferrugineus* Roxb showed moderate cytotoxic activity against cervical cancer (HeLa) and lung cancer (A549) cell lines, with IC_{50} values of 47.62 µg/mL and 192.83 µg/mL, respectively. Similarly, the acetone extract of *C. sappan* L showed moderate activity against A549 cells, with an IC_{50} value of 90.01 µg/mL.[4]

These outcomes align with the phytochemical profiles of each extract. *C. sappan* contains the homoisoflavonoid brazilin (Figure 7), which has been repeatedly associated with antiproliferative and pro-apoptotic effects in multiple tumor models, including breast cancer.[42] *L. ferrugineus* provides the flavonoids quercetin, quercitrin, 4″-O-acetylquercitrin (Figure 8), tannins, and alkaloids, with quercetin reported to induce apoptosis and modulate oncogenic signaling.[10,43]

Flavonoids inhibit cancer cell progression through multiple, complementary mechanisms, including growth suppression, protein-kinase signaling inhibition, apoptosis induction, downregulation of matrix metalloproteinase secretion with consequent blockade of invasion, interference with cell adhesion and spreading, and anti-angiogenic activity.[44–46]

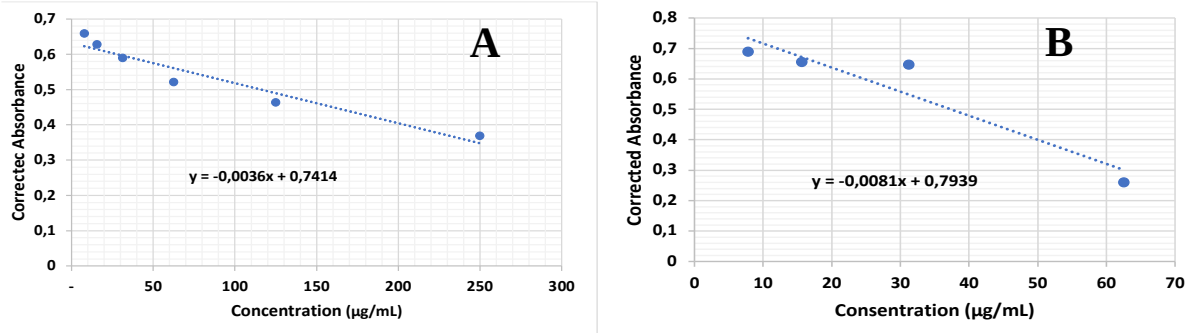

Figure 5. Resazurin Linear regression plots used for IC_{50} determination: (a) *L. ferrugineus* (acetone extract); (b) *C. sappan* (acetone extract).

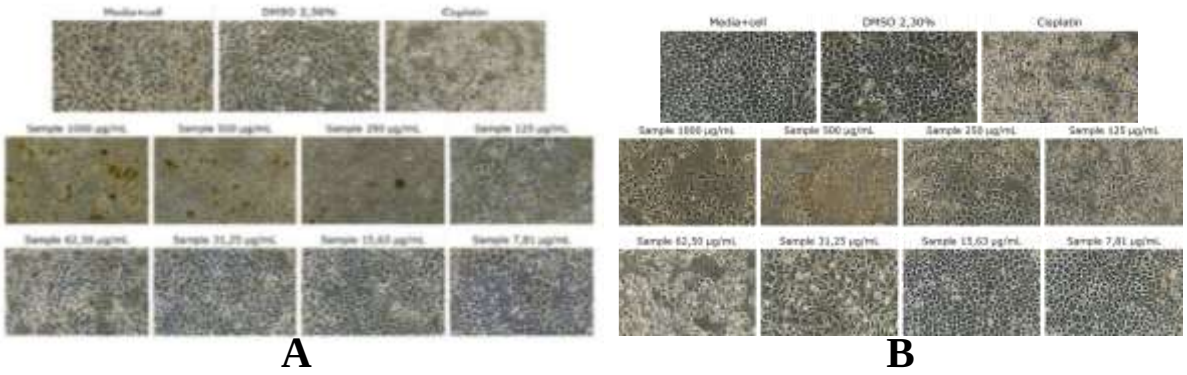

Figure 6. Representative phase-contrast micrographs of MCF-7 morphology after treatment with single extracts: (a) *L. ferrugineus*; (b) *C. sappan*.

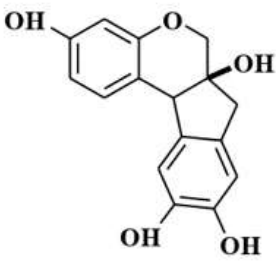

Figure 7. Structure of Brazilin

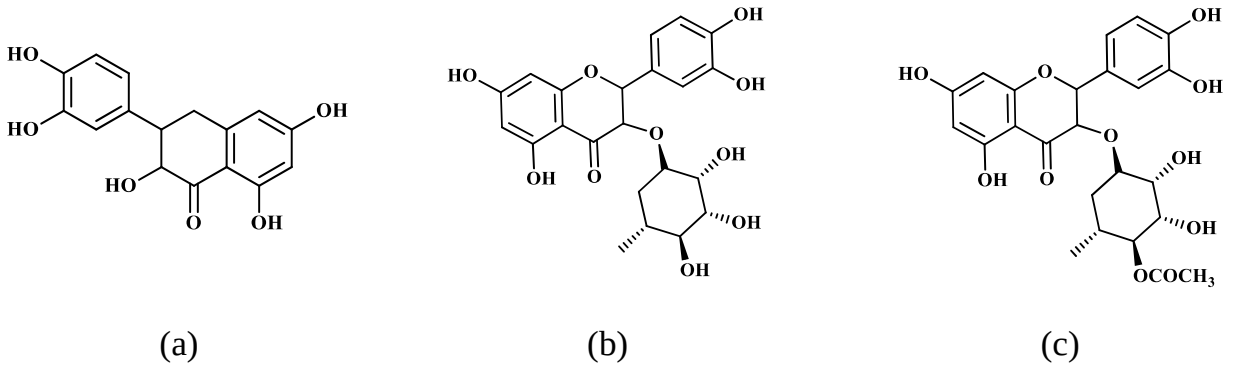

Figure 8. Structures of Quercetin (a), Quercitrin (b), and 4″-O-Acetylquercitrin (c)

Binary mixtures of *L. ferrugineus:C. sappan* at 1:1, 2:1, and 1:2 (Figure 9a–c) yielded IC_{50} values of 102.03, 114.35, and 104.28 µg/mL, respectively; thus, they are inactive by the stated criteria and notably less potent than the single *C. sappan* extract. Such reduced efficacy is consistent with the combination-effect theory, wherein bioactive agents with overlapping targets or convergent mechanisms may compete for the same cellular binding sites, producing antagonism that diminishes the overall activity compared with either agent alone, as reflected in the right-shifted IC_{50} curves of the mixtures.[47] Although the IC_{50} values for all three extract combinations exceeded 100 µg/mL, morphological assessment (Figure 10) at 62.50 µg/mL still revealed extensive MCF-7 cell death evidenced by reduced viable-cell density, loss of bright nuclear staining, overt membrane disruption, and an overall phenotype closely resembling cisplatin-treated cells.

At 62.50 µg/mL, combination-treated cultures (Figure 10a–c) showed reduced viable morphology; however, the effect size did not translate to IC_{50} values comparable with the single *C. sappan* extract, again compatible with antagonistic interactions rather than additivity/synergy. Docking of the single ligands indicated favorable CYP3A4 binding for quercetin and brazilin, with quercetin showing the most negative ΔG and a denser hydrogen-bond/hydrophobic network near THR310, ALA370, and CYS442. Because the experimental mixtures are not a new chemical entity, concurrent exposure likely promotes competition for overlapping binding environments and/or metabolic interference, thereby diminishing functional target engagement and producing the right-shifted (higher) IC_{50} values observed for the combinations. Consistent with this interpretation, the QSAR screen (Table 3) indicates that any conceptual "combined" construct would be excessively large and suboptimally partitioned, limiting cellular uptake and clear potency.[48] Taken together, the *in silico* and *in vitro* results support a competitive antagonism model in which the two actives vie for similar sites within the same receptor environment, with a concentration-dependent net effect.

Combination effects

One therapeutic strategy to achieve effective and safe cancer treatment is combination therapy with anticancer agents. Combinations may pair a conventional chemotherapeutic with a natural product or two natural products. In this study, we evaluated a natural–natural combination using the acetone extracts of *L. ferrugineus* and *C. sappan*. Both botanicals have demonstrated anticancer activity in previous studies. The IC_{50} values for the binary mixtures (1:1, 2:1, and 1:2, w/w) were determined from the linear regression of the dose–response curves shown in Figure 9.

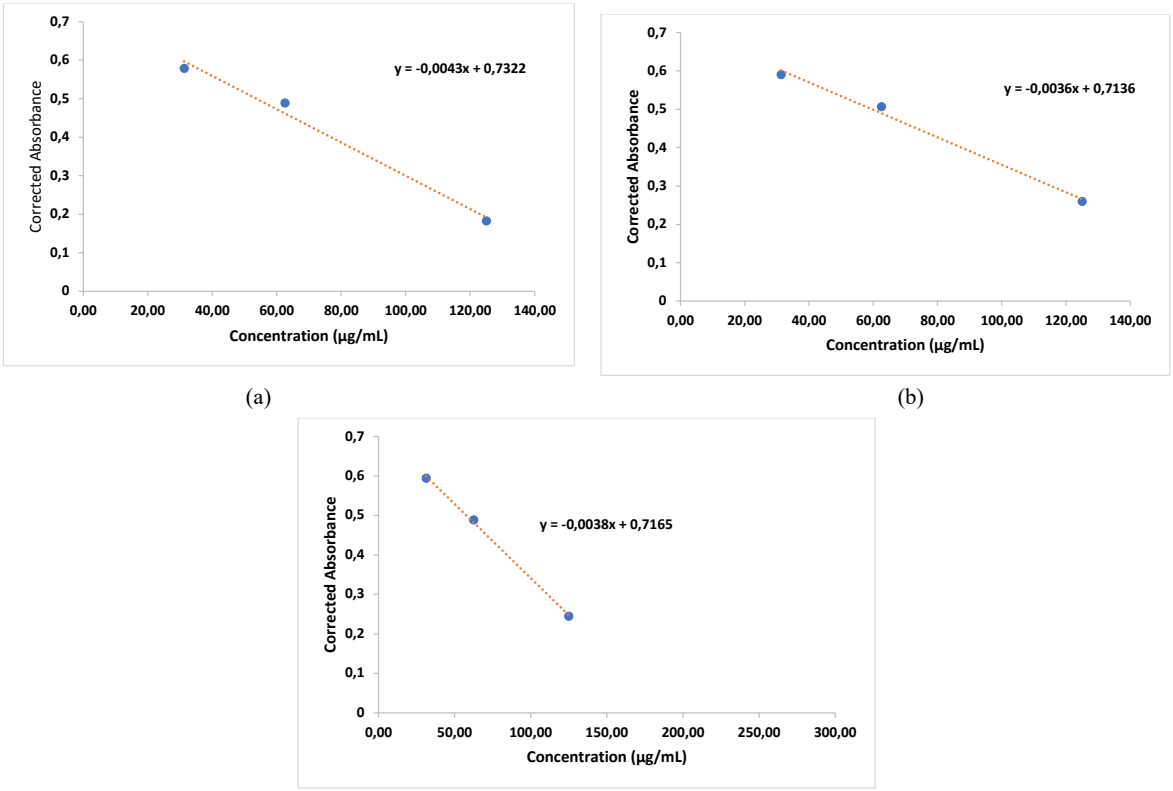

Figure 9. Linear regression plots for binary mixtures of *L. ferrugineus:C. sappan*: (a) 1:1; (b) 2:1; (c) 1:2.

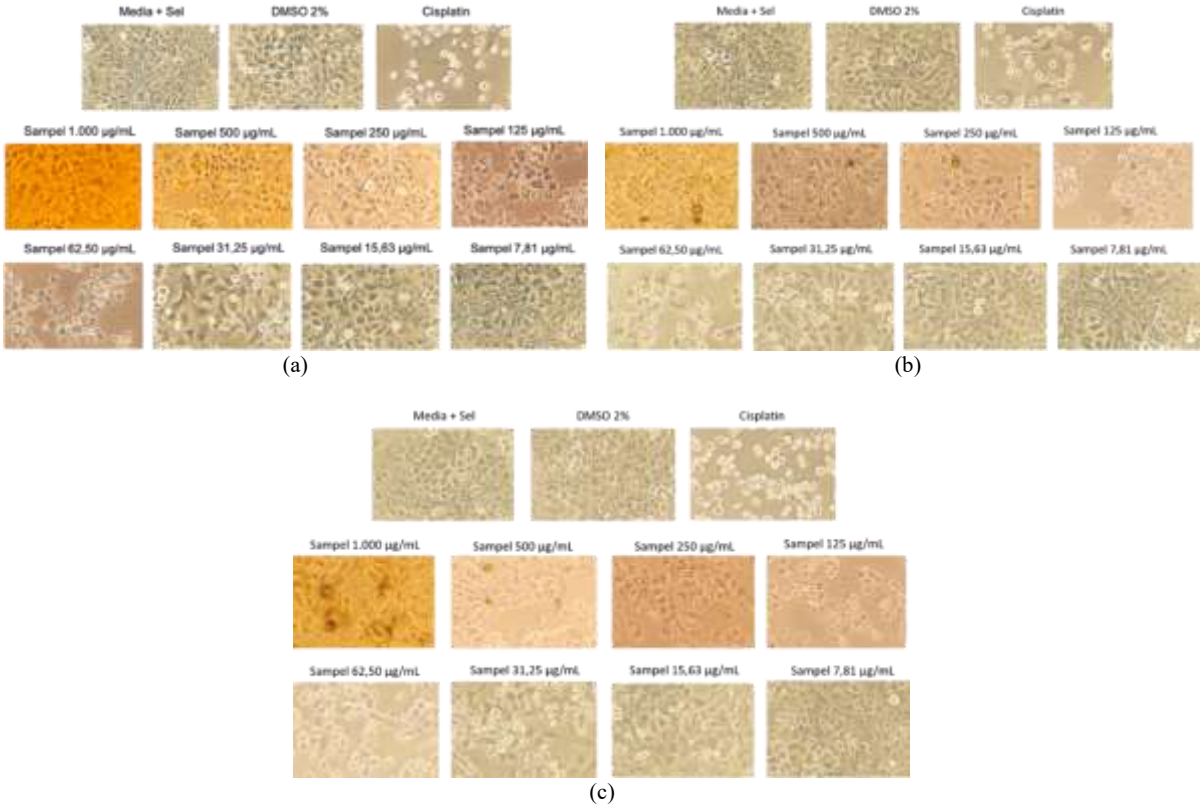

Figure 10. MCF-7 morphology after treatment with *L. ferrugineus* : *C. sappan* mixtures at 62.50 µg/mL: (a) 1:1; (b) 2:1; (c) 1:2.

Table 3. Table of QSAR variable analysis results for the ligands quercetin, brazilin, and their Combination

Parameter	Quercetin	Brazilin	Brazilin + Quercetin	Natural Ligands (1TQN)
Surface Area (Grid, Å²)	445.43	454.31	769.10	798.45
Volume (Å³)	711.14	750.32	1329.11	1452.94
Hydration Energy	−27.71	−25.11	−40.74	−19.50
log P	3.30	1.69	4.00	4.78
Refractivity (Å³)	38.37	30.98	76.39	61.26
Polarizability (Å³)	25.17	29.07	50.44	44.22
Mass (amu)	280.19	286.28	555.39	586.26

Conclusion

C. sappan acetone extract showed moderate cytotoxicity against MCF-7 breast cancer cells (IC_{50} = 56.21 µg/mL) and favorable *in silico* binding to CYP3A4 via brazilin, supporting its potential as an anticancer lead. In contrast, the *L. ferrugineus* extract was inactive in this model (IC_{50} = 112.9 µg/mL), despite the strong *in silico* interaction profile of quercetin. Notably, the binary mixtures of *L. ferrugineus*:*C. sappan* (1:1, 2:1, and 1:2) yielded IC_{50} values >100 µg/mL and attenuated the morphological effects relative to the single *C. sappan* extract, indicating loss of efficacy upon combination. This outcome does not support the initial synergy hypothesis but instead underscores the importance of a mechanism-aware combination design for botanical agents. Future work should prioritize delivery optimization to address physicochemical liabilities while maintaining the extracts as separate entities rather than a merged ligand to clarify whether formulation or scheduling can recover efficacy without reintroducing antagonism.

Conflict of Interest

The author`s declare no conflicts of interest.

Authors' Declaration

The authors hereby declare that the work presented in this article is original and that any liability for claims relating to the content of this article will be borne by them.

Acknowledgements

This work was supported by the Non-Tax State Revenue (PNBP) funds of Universitas Negeri Medan for Fiscal Year 2024, in accordance with the Rector's Decree of Universitas Negeri Medan No. 00299/UN33/KPT/2024.

Reference

1. Bray F, Laversanne M, Sung H, Ferlay J, Siegel RL, Soerjomataram I, Jemal A. Global cancer statistics 2022: GLOBOCAN estimates of incidence and mortality worldwide for 36 cancers in 185 countries. CA Cancer J Clin. 2024;74(3):229-263. Doi:10.3322/caac.21834
2. Saini A, Kumar M, Bhatt S, Saini V, Malik A. Cancer Causes and Treatments. Int J Pharm Sci Res. 2020;11(7):3109. Doi:10.13040/IJPSR.0975-8232.11(7).3109-22
3. Tubin S, Vozenin MC, Prezado Y, Durante M, Prise KM, Lara PC, Greco C, Massaccesi M, Guha C, Wu X, Mohiuddin MM, Vestergaard A, Bassler N, Gupta S, Stock M, Timmerman R. Novel unconventional radiotherapy techniques: Current status and future perspectives – Report from the 2nd international radiation oncology online seminar. Clin Transl Radiat Oncol. 2023;40:100605. Doi:10.1016/j.ctro.2023.100605
4. Juwitaningsih T, Syahputra N, Eddiyanto E, Windayani N, Rukayadi Y. Antibacterial and Anticancer Activities of Acetone Extract *Caesalpinia sappan* L. al-Kimiya. 2023;9(2):82-88. Doi:10.15575/ak.v9i2.20966
5. Suyatmi S, Mudigdo A, Purwanto B, Indarto D, Hakim F, Krisnawati D. Brazilin Isolated from *Caesalpina Sappan* Wood Induces Intrinsic Apoptosis on A549 Cancer Cell Line by Increasing p53, caspase-9, and caspase-3. Asian Pac J Cancer Prev. 2022;23(4):1337-1343. Doi:10.31557/APJCP.2022.23.4.1337
6. Astirin OP, Artanti AN, Herawati E, Putri FA, Muhyidin MF, Prihapsara F. Cytotoxic effects of fractions, isolates, and nanoparticles of soursop leaf (*Annona muricata* L.) and sappan wood (*Caesalpinia sappan* L.) against human cervical cancer HeLa cells. Indian J Nat Prod Resour. Published online 2023. Doi:10.56042/ijnpr.v14i4.5779
7. Yang X, Liang Y, Zhao L, Chen L, Yang Y, Wang J, Yan L, Zhang S, Liu X, Zhang H. Brazilin Inhibits the Invasion and Metastasis of Breast Cancer. Biol Pharm Bull. 2023;46(6):b22-00637. Doi:10.1248/bpb.b22-00637
8. Jeong M, Chun J, Park SM, Yeo H, Na SW, Ha IJ, Kim B, Jeong MK. An Investigation of the Anticancer Mechanism of *Caesalpinia sappan* L. Extract Against Colorectal Cancer by Integrating a Network Pharmacological Analysis and Experimental Validation. Plants. 2025;14(2):263. Doi:10.3390/plants14020263
9. Juwitaningsih T, Roza D, Silaban S, Hermawati E, Windayani N. Phytochemical screening, antibacterial, antioxidant, and anticancer activity of Coffee parasite acetone extract (*Loranthus ferrugineus* Roxb). Pharmacia. 2022;69(4):1041-1046. Doi:10.3897/pharmacia.69.e91427
10. Nigam YP. The Bornean Mistletoes as Versatile Parasites: A Systematic Review. Sys Rev Pharm. 2022; 13(1): 42-47. Doi:10.31858/0975-8453.13.1.42-47
11. Niazvand F, Orazizadeh M, Khorsandi L, Abbaspour M, Mansouri E, Khodadadi A. Effects of Quercetin-Loaded Nanoparticles on MCF-7 Human Breast Cancer Cells. Medicina (B Aires). 2019;55(4):114. Doi:10.3390/medicina55040114
12. Suyatmi S, Mudigdo A, Purwanto B, Indarto D, Hakim F, Krisnawati D. Brazilin Isolated from *Caesalpina Sappan* Wood Induces Intrinsic Apoptosis on A549 Cancer Cell Line by Increasing p53, caspase-9, and caspase-3. Asian Pac J Cancer Prev. 2022;23(4):1337-1343. Doi:10.31557/APJCP.2022.23.4.1337
13. Dewi Harnis AP, A.H.M. Hasan N, Janah YK, Tsamara CA, Fatchiyah F. Virtual Inhibition Analysis of Bioactive Compound Brazilin (*Caesalpinia sappan* L.) Toward Progesterone Receptor or Lonaprisan in Breast Cancer Proliferation. Biotrop: j. tropical biol. 2020;8(2):62-70. doi:10.21776/ub.biotropika.2020.008.02.01
14. Tirtanirmala P, Novarina A, Utomo RY, Sugiyanto RN, Jenie RI, Meiyanto E. Cytotoxic and Apoptotic-inducing Effect of Fraction Containing Brazilein from *Caesalpinia sappan* L. and Cisplatin on T47D Cell Lines. Indones. J. Cancer Chemoprevention. 2017;6(3):89-96. Doi:10.14499/indonesianjcanchemoprev6iss3pp89-96
15. Thomaz DV, Rodrigues ESB, Machado FB, Macedo IYL. Investigation of Cyclobenzaprine Interactions with P450 Cytochromes CYP1A2 and CYP3A4 through Molecular Docking Tools. Path Sci. 2019;5(2):4001-4006. Doi:10.22178/pos.43-1
16. Gor PP, Su HI, Gray RJ, Gimotty PA, Horn M, Aplenc R, Vaughan WP, Tallman MS, Rebbeck TR, DeMichele A. Cyclophosphamide- metabolizing enzyme polymorphisms and

survival outcomes after adjuvant chemotherapy for node-positive breast cancer: a retrospective cohort study. Breast Cancer Res. 2010;12(3):R26. Doi:10.1186/bcr2570
17. El-Serafi I, Steele S. Cyclophosphamide Pharmacogenomic Variation in Cancer Treatment and Its Effect on Bioactivation and Pharmacokinetics. Adv Pharmacol Pharm Sci. 2024;2024:4862706. Doi:10.1155/2024/4862706
18. Muthi I, Riris Istighfari J, Rohmad Yudi U, Nur Dina A, Gagas Pradani Nur I, Masashi K, Edy M. Genistein enhances cytotoxic and antimigratory activities of doxorubicin on 4T1 breast cancer cells through cell cycle arrest and ROS generation. J Appl Pharm Sci. 2020;10(10):095-104. Doi:10.7324/JAPS.2020.1010011
19. Mahmoud AM, El-Shemy HA. Efficacy Assessment for Several Natural Products with Potential Cytotoxic Activity Against Breast and Cervix Cancers. J. Arid. Land. 2012;22(1):107-110.
20. Zubair MS, Anam S, Maulana S, Arba M. *In Vitro* and *In Silico* Studies of Quercetin and Daidzin as Selective Anticancer Agents. Indones. J. Chem. 2021;21(2):310-317. Doi:10.22146/ijc.53552
21. Tang SM, Deng XT, Zhou J, Li QP, Ge XX, Miao L. Pharmacological basis and new insights of quercetin action in respect to its anti-cancer effects. Biomed Pharmacother. 2020;121:109604. Doi:10.1016/j.biopha.2019.109604
22. Biswas P, Dey D, Biswas PK, Rahaman TI, Saha S, Parvez A, Khan DA, Lily NJ, Saha K, Sohel M, Hasan MM, Al Azad S, Bibi S, Hasan MN, Rahmatullah M, Chun J, Rahman MA, Kim B. A Comprehensive Analysis and Anti-Cancer Activities of Quercetin in ROS-Mediated Cancer and Cancer Stem Cells. Int J Mol Sci. 2022;23(19). Doi:10.3390/ijms231911746
23. Forli S, Huey R, Pique ME, Sanner MF, Goodsell DS, Olson AJ. Computational protein–ligand docking and virtual drug screening with the AutoDock suite. Nat Protoc. 2016;11(5):905-919. Doi:10.1038/nprot.2016.051
24. Lavogina D, Lust H, Tahk MJ, Laasfeld T, Vellama H, Nasirova N, Vardja M, Eskla KL, Salumets A, Rinken A, Jaal J. Revisiting the Resazurin-Based Sensing of Cellular Viability: Widening the Application Horizon. Biosensors (Basel). 2022;12(4):196. doi:10.3390/bios12040196
25. Susianti S, Lesmana R, Salam S, Julaeha E, Pratiwi YS, Sylviana N, Goenawan H, Kurniawan A, Supratman U. The Effect of Nutmeg Seed (*M. fragrans*) Extracts Induces Apoptosis in Melanoma Maligna Cell's (B16-F10). Indones. Biomed. J.. 2021;13(1):68-74. Doi:10.18585/inabj.v13i1.1424
26. Lipinski CA, Lombardo F, Dominy BW, Feeney PJ. Experimental and computational approaches to estimate solubility and permeability in drug discovery and development settings 1PII of original article: S0169-409X(96)00423-1. Adv Drug Deliv Rev. 2001;46(1-3):3-26. Doi:10.1016/S0169-409X(00)00129-0
27. Daina A, Michielin O, Zoete V. SwissADME: a free web tool to evaluate pharmacokinetics, drug-likeness and medicinal chemistry friendliness of small molecules. Sci Rep. 2017;7(1):42717. Doi:10.1038/srep42717
28. Trott O, Olson AJ. AutoDock Vina: Improving the speed and accuracy of docking with a new scoring function, efficient optimization, and multithreading. J Comput Chem. 2010;31(2):455-461. Doi:10.1002/jcc.21334
29. Roza D, Fadhilah G, Indriani E, Wiliranti YA, Juwitaningsih T. Evaluation of Anticancer and Antioxidant Activities (*In Vitro* Studies) of Coffee Stem Parasite Extract [*Scurrula ferruginea* (Roxb. ex Jack) Danser] and *In Silico* Studies of its Isolate. Turk J Pharm Sci. 2024;21(5):463-473. Doi:10.4274/tjps.galenos.2023.26243
30. Karami TK, Hailu S, Feng S, Graham R, Gukasyan HJ. Eyes on Lipinski's Rule of Five: A New "Rule of Thumb" for Physicochemical Design Space of Ophthalmic Drugs. J Ocul Pharmacol Ther. 2022;38(1):43-55. Doi:10.1089/jop.2021.0069
31. Yano JK, Wester MR, Schoch GA, Griffin KJ, Stout CD, Johnson EF. The Structure of Human Microsomal Cytochrome P450 3A4 Determined by X-ray Crystallography to 2.05-Å Resolution. J. biol. chem. 2004;279(37):38091-38094. Doi:10.1074/jbc.C400293200
32. Ekroos M, Sjögren T. Structural basis for ligand promiscuity in cytochrome P450 3A4. Proc Natl Acad Sci U S A. 2006;103(37):13682-13687. Doi:10.1073/pnas.0603236103
33. Tang H, Kuang Y, Wu W, Peng B, Fu Q. Quercetin inhibits the metabolism of arachidonic acid by inhibiting the activity of CYP3A4, thereby inhibiting the progression of breast cancer. Mol Med. 2023;29(1):127. Doi:10.1186/s10020-023-00720-8
34. Trott O, Olson AJ. AutoDock Vina: Improving the speed and accuracy of docking with a new scoring function, efficient optimization, and multithreading. J Comput Chem. 2010;31(2):455-461. Doi:10.1002/jcc.21334
35. Kiani YS, Ranaghan KE, Jabeen I, Mulholland AJ. Molecular Dynamics Simulation Framework to Probe the Binding Hypothesis of CYP3A4 Inhibitors. Int J Mol Sci. 2019;20(18):4468. Doi:10.3390/ijms20184468
36. Ridhwan MJM, Bakar SIA, Latip NA, Ghani NA, Ismail NH. A Comprehensive Analysis of Human CYP3A4 Crystal Structures as a Potential Tool for Molecular Docking-Based Site of Metabolism and Enzyme Inhibition Studies. J Comput Biophys Chem. 2022;21(03):259-285. Doi:10.1142/S2737416522300012
37. Wang J, Nithianantham S, Chai SC, Jung YH, Yang L, Ong HW, Li Y, Zhang Y, Miller DJ, Chen T. Decoding the selective chemical modulation of CYP3A4. Nat Commun. 2025;16(1):3423. Doi:10.1038/s41467-025-58749-8
38. Dhiman N, Awasthi R, Sharma B, Kharkwal H, Kulkarni GT. Lipid Nanoparticles as Carriers for Bioactive Delivery. Front Chem. 2021;9. Doi:10.3389/fchem.2021.580118
39. Pinheiro RGR, Pinheiro M, Neves AR. Nanotechnology Innovations to Enhance the Therapeutic Efficacy of Quercetin. Nanomaterials. 2021;11(10):2658. Doi:10.3390/nano11102658
40. Lavogina D, Lust H, Tahk MJ, Laasfeld T, Vellama H, Nasirova N, Vardja M, Eskla KL, Salumets A, Rinken A, Jaal J. Revisiting the Resazurin-Based Sensing of Cellular Viability: Widening the Application Horizon. Biosensors (Basel). 2022;12(4). Doi:10.3390/bios12040196
41. Pezzuto JM, Song LL, Lee SK, Shamon LA, Mata-Greenwood E, Jang M, Jeong HJ, Pisha E, Mehta RG, Kinghorn AD. Bioassay Methods Useful for Activity-Guided Isolation of Natural Product Cancer Chemopreventive Agents. In: Chemistry, Biological and Pharmacological Properties of Medicinal Plants from the Americas. Routledge; 2018:81-110. Doi:10.1201/9781315139272-5
42. Juwitaningsih T, Jahro IS, Sari SA. Evaluation of North Sumatera Cardamom seed (*Amomum compactum*) Extract as Antibacterial and Anticancer. J Phys Conf Ser. 2020;1485(1):012019. doi:10.1088/1742-6596/1485/1/012019
43. Kumal K, Pant DR, Aryal B, Tripathi GR, Joshi GP. Phytochemical and Antioxidant Properties Of Traditionally Used Mistletoes In Nepal. Sci World. 2021;14(14):83-89. Doi:10.3126/sw.v14i14.34999
44. Chatterjee B, Ghosh K, Swain A, Nalla KK, Ravula H, Pan A, Kanade SR. The phytochemical brazilin suppress DNMT1 expression by recruiting p53 to its promoter resulting in the epigenetic restoration of p21 in MCF7cells. Phytomedicine. 2022;95:153885. Doi:10.1016/j.phymed.2021.153885
45. Kopustinskiene DM, Jakstas V, Savickas A, Bernatoniene J. Flavonoids as Anticancer Agents. Nutrients. 2020;12(2):457. Doi:10.3390/nu12020457
46. Engel N, Oppermann C, Falodun A, Kragl U. Proliferative effects of five traditional Nigerian medicinal plant extracts on human breast and bone cancer cell lines. J Ethnopharmacol. 2011;137(2):1003-1010. Doi:10.1016/j.jep.2011.07.023
47. Tang J, Wennerberg K, Aittokallio T. What is synergy? The Saariselkä agreement revisited. Front Pharmacol. 2015;6(181). Doi:10.3389/fphar.2015.00181
48. Canga I, Vita P, Oliveira AI, Castro MÁ, Pinho C. *In Vitro* Cytotoxic Activity of African Plants: A Review. Molecules. 2022;27(15). Doi:10.3390/molecules27154989